Ann. Appl. Math.
doi: 10.4208/aam.OA-2023-0017

Vol. **39**, No. 3, pp. 264-280
August 2023

An Iterative Thresholding Method for the Heat Transfer Problem

Luyu Cen[1] and Xiaoping Wang[1,2,3,*]

[1] *Department of Mathematics, Hong Kong University of Science and Technology, Clear Water Bay, Kowloon, Hong Kong, China*
[2] *School of Science and Engineering, The Chinese University of Hong Kong, Shenzhen, Guangdong 518172, China*
[3] *Shenzhen International Center for Industrial and Applied Mathematics, Shenzhen Research Institute of Big Data, Shenzhen, Guangdong 518172, China*

Received 24 May 2023; Accepted (in revised version) 27 July 2023

Dedicated to the memory of Professor Zhongci Shi

Abstract. In this paper, we propose a simple energy decaying iterative thresholding algorithm to solve the heat transfer problem. The material domain is implicitly represented by its characteristic function, and the problem is formulated into a minimum-minimum problem. We prove that the energy is decreasing in each iteration. Numerical experiments for two types the heat transfer problems (volume to point and volume to sides) are performed to demonstrate the effectiveness of the proposed methods.

AMS subject classifications: 80M50, 74B05, 74P15

Key words: Optimization in heat transfer, convolution, thresholding.

1 Introduction

Topology optimization has been widely applied to the design of heat transfer systems to improve their performance while minimizing material usage and manufacturing

*Corresponding author.
Emails: lcen@connect.ust.hk (L. Cen), mawang@ust.hk (X. Wang)

costs [1, 7, 14, 19, 21]. Thermal management of electronic components involves controlling their temperature to ensure that they operate within safe limits and perform optimally. Electronic components generate heat during operation, and if the heat is not dissipated efficiently, it can lead to premature failure or reduced performance. Effective thermal management is critical for the performance and reliability of electronic components, particularly in high-power applications such as data centers [18], power electronics [15], and electric vehicles [17, 20].

Topology optimization methods can be used to design heat sinks and other cooling devices that are highly optimized for thermal management. These methods can help to improve the performance and efficiency of electronic components and other thermal management systems, while also reducing their size and weight. There are several different topology optimization methods that can be used for thermal management, including density-based methods which use a density function to represent the material distribution within the heat transfer devices and update the density function iteratively to optimize the material distribution for maximum heat transfer efficiency [2,3,8,11,24]; level set methods which use a level set function to represent the geometry of thermal conductive material [13, 25]. See [6, 10] for reviews.

Among the various methods used for topology optimization, the threshold dynamics method [9, 16] has recently gained attention due to its ability to handle complex and nonlinear problems with high computational efficiency. The threshold dynamics method is a mathematical framework for topology optimization based on iteratively updating a characteristic function which separates the design domain into two regions. The method has been successfully applied to various engineering problems, including image segmentation [22, 23], fluid channel design [5], flow network design [12], minimum compliance problem [4], by optimizing the characteristic function to achieve a desired performance objective.

In this paper, we present a novel application of the threshold dynamics method to topology optimization of heat transfer systems. We focus on the implementation of the method and its performance in optimizing the thermal performance of heat transfer systems. Specifically, we demonstrate the effectiveness of the method in improving the heat transfer rate and reducing thermal resistance by optimizing the topology of heat transfer components.

To achieve this, we start by introducing the conductive steady-steate heat transfer problem defined by Bejan [2]. The problem represents an electrical device that is cooled down by a limited amount of high conductive material aiming at driving the produced heat to a heat sink, located at the boundary of the finite size volume. We then formulate the optimization problem in terms of characterization function of the domain and design a threshold dynamics method to solve the problem. We present the results of our numerical simulations, demonstrating the effectiveness of

the threshold dynamics method in optimizing the topology of heat transfer systems. We discuss the implications of our findings and outline the potential for further research in this area.

2 Problem formulation

Consider the steady-state heat transfer problem on a two-dimensional domain studied by Bejan [2]:

$$-\nabla\cdot(k\nabla T)=q \quad \text{on} \quad \Omega, \tag{2.1a}$$
$$(k\nabla T)\cdot\mathbf{n}=0 \quad \text{on} \quad \Gamma\backslash\Gamma_D, \tag{2.1b}$$
$$T=T_0 \quad \text{on} \quad \Gamma_D, \tag{2.1c}$$

where T is temperature with unit K, q is heat generation rate per unit volume with unit W/m^3, and k is thermal conductivity with unit W/mK. As in [2], we assume that the volume generates heat uniformly and thus q is constant. Two kinds of material with different thermal conductivity k_0,k_1,$k_1>>k_0$ distribute over Ω. Let χ be the characteristic function indicating the domain with high thermal conductivity

$$\chi(\mathbf{x})=\begin{cases} 1, & k(\mathbf{x})=k_1, \\ 0, & k(\mathbf{x})=k_0. \end{cases}$$

Then

$$k(\chi)=k_0+(k_1-k_0)\chi. \tag{2.2}$$

The problem is to design the optimal heat conducting paths to minimize the average temperature over Ω subject to a limited amount of high thermal conductive material. The optimization problem is

$$\min_{\chi,T}\frac{1}{|\Omega|}\int_\Omega T d\mathbf{x} \tag{2.3}$$

subject to

$$\int_\Omega \chi d\mathbf{x}\le V$$
$$-\nabla\cdot(k(\chi)\nabla T)=q \quad \text{on} \quad \Omega,$$
$$(k(\chi)\nabla T)\cdot\mathbf{n}=0 \quad \text{on} \quad \Gamma\backslash\Gamma_D,$$
$$T=T_0 \quad \text{on} \quad \Gamma_D.$$

Multiplying $T-T_0$ to both sides of (2.1b) and integrating by parts, we have

$$\int_\Omega q(T-T_0)d\mathbf{x}=\int_\Omega k(\chi)|\nabla T|^2 d\mathbf{x}.$$

Therefore, minimizing the average temperature (when q is a constant) is equivalent to minimizing the heat dissipation which is the right hand side of the above equation. In developing an optimization algorithm, instead of updating χ and T simultaneously, it is easier to update T by solving the steady-state equation when χ is given. We would like to seek an equivalent formulation of the above optimization problem so that solving the steady state equation would minimize an energy given χ and then χ could be updated to minimize the same energy again with T fixed.

Lemma 2.1. *Let T be the solution to* (2.1b) *and denote $\mathbf{R}^*=k\nabla T$, then*

$$\mathbf{R}^*\in\underset{\mathbf{R}\in S}{\arg\min}\int_\Omega\frac{1}{k}\mathbf{R}\cdot\mathbf{R}d\mathbf{x},$$

where

$$S:=\{\mathbf{R}:\Omega\to\mathbb{R}^2:-\nabla\cdot\mathbf{R}=q,\ \mathbf{R}\cdot\mathbf{n}=0\ on\ \Gamma\backslash\Gamma_D\}.$$

Remark 2.1. The set S can be seen as the admissible heat flux set (or more precisely, admissible negative heat flux set). If $\tilde{T}$ is the solution to the heat transfer equation with an arbitrary heat conductivity distribution $\tilde{k}$, that is, if $-\nabla\cdot(\tilde{k}\nabla\tilde{T})=0$, $\tilde{k}\nabla\tilde{T}\cdot\mathbf{n}=0$ on $\Gamma\backslash\Gamma_D$ and an arbitrary boundary condition on Γ_D, it would be easy to see that $\tilde{\mathbf{R}}=\tilde{k}\nabla\tilde{T}\in S$. This lemma shows that the minimizer to $\int_\Omega\frac{1}{k}\mathbf{R}\cdot\mathbf{R}d\mathbf{x}$ among all admissible negative heat flux, is exactly $k\nabla T$, which is the negative heat flux of T that solves the heat equation with heat conductivity k with a constant Dirichlet condition on Γ_D.

The proof of the lemma is given in Appendix.

Let

$$B:=\left\{\chi:\Omega\to\{0,1\};\int_\Omega\chi d\mathbf{x}\le V\right\}.$$

Since the thermal conductivity $k(\chi)$ is a piece-wise constant function, then

$$\frac{1}{k(\chi)}=\frac{1}{k_0}+\left(\frac{1}{k_1}-\frac{1}{k_0}\right)\chi.$$

We apply a convolution to χ to smooth the function

$$\frac{1}{k(G_\sigma*\chi)}=\frac{1}{k_0}+\left(\frac{1}{k_1}-\frac{1}{k_0}\right)G_\sigma*\chi,$$

where

$$G_\sigma=\frac{1}{2\pi\sigma^2}e^{\frac{-||\mathbf{x}||^2}{2\sigma^2}}.$$

Denote

$$\mathcal{J}(\chi,\mathbf{R}):=\int_\Omega \frac{1}{k(G_\sigma*\chi)}\mathbf{R}\cdot\mathbf{R}d\mathbf{x}. \tag{2.4}$$

Problem (2.3) is then reformulated as

$$\min_{\chi\in B}\min_{\mathbf{R}\in S}\mathcal{J}(\chi,\mathbf{R}). \tag{2.5}$$

3 A thresholding algorithm

For this min-min problem (2.5), we can design a coordinate descent algorithm which alternately finds the descent direction of one variable while fixing the other variable. Given an initial guess χ^0, we update $\mathbf{R}$ and χ in the following order,

$$\mathbf{R}^0,\chi^1,\mathbf{R}^1,\cdots,\mathbf{R}^m,\chi^{m+1},\cdots,$$

where

$$\mathbf{R}^m=\arg\min_{\mathbf{R}\in S}\mathcal{J}(\chi^m,\mathbf{R}), \tag{3.1a}$$

$$\chi^{m+1}=\arg\min_{\chi\in B}\mathcal{J}(\chi,\mathbf{R}^m). \tag{3.1b}$$

The algorithm goes as follows

Algorithm 3.1.

Input: σ,V,k_1,k_0 and initial guess χ^0 with $\int_\Omega\chi=V$.
$m\leftarrow 0$
repeat
  $\rho\leftarrow G_\sigma*\chi^m$
  $k(G_\sigma*\chi^m)\leftarrow\frac{1}{(\frac{1}{k_1}-\frac{1}{k_0})G_\sigma*\chi^m+\frac{1}{k_0}}$
  Solve (2.1b) with $k=k(G_\sigma*\chi^m)$ for T^m
  $\mathbf{R}^m\leftarrow k(G_\sigma*\chi^m)\nabla T^m$
  $\phi^m\leftarrow G_\sigma*\left[\left(\frac{1}{k_1}-\frac{1}{k_0}\right)\mathbf{R}^m\cdot\mathbf{R}^m\right]$
  $\delta\leftarrow\sup\{a:|\{\mathbf{x}\in\Omega:\phi^m(\mathbf{x})<a\}|\le V\}$
  $\tilde{A}_\delta\subset\{\mathbf{x}\in\Omega:\phi^k(x)=\delta\}$ and $|\tilde{A}_\delta|=V-|\{\mathbf{x}\in\Omega:\phi^k(\mathbf{x})<\delta\}|$
  $\chi^{m+1}(\mathbf{x})\leftarrow 1$ if $\phi^m(\mathbf{x})<\delta$ or $\mathbf{x}\in\tilde{A}_\delta$
  $\chi^{m+1}(\mathbf{x})\leftarrow 0$ otherwise
  $m\leftarrow m+1$
until convergence

4 Energy decaying property

In this section, we show that Algorithm 3.1 designed above has the energy decaying property.

Lemma 4.1. *Given ϕ^m, let us denote δ by*

$$\delta=\sup\{a:|\{\mathbf{x}\in\Omega:\phi^m(\mathbf{x})<a\}|\leq V\}. \tag{4.1}$$

We define

$$\chi^{m+1}=\begin{cases} 1, & \phi^m<\delta \quad or \quad \mathbf{x}\in\tilde{A}_\delta, \\ 0, & otherwise, \end{cases} \tag{4.2}$$

where $\tilde{A}_\delta$ is any subset of the level set $\{x\in\Omega:\phi^k(\mathbf{x})=\delta\}$ and $|\tilde{A}_\delta|=V-|\{\mathbf{x}\in\Omega:\phi^k(\mathbf{x})<\delta\}|$. Then $\int_\Omega\chi^{m+1}d\mathbf{x}=V$ and

$$\int_\Omega\chi^{m+1}\phi^m d\mathbf{x}-\int_\Omega\chi\phi^m d\mathbf{x}\leq 0, \quad \forall\chi\in B \quad with \quad \int_\Omega\chi d\mathbf{x}=V.$$

Moreover, if $\delta\leq 0$,

$$\int_\Omega\chi^{m+1}\phi^m d\mathbf{x}-\int_\Omega\chi\phi^m d\mathbf{x}\leq 0, \quad \forall\chi\in B,$$

that is,

$$\chi^{m+1}=\operatorname*{argmin}_{\chi\in B}\int_\Omega\chi\phi^m d\mathbf{x}.$$

Proof. First, we show that $|\{\mathbf{x}\in\Omega:\phi<\delta\}|\leq V$ and $|\{\mathbf{x}\in\Omega:\phi\leq\delta\}|\geq V$. There exists $\delta_1\leq\delta_2\leq\cdots\leq\delta_n\leq\cdots$, $\delta_n\to\delta$, and $|\{\mathbf{x}\in\Omega:\phi^m<\delta_n\}|\leq V$. Since $\{\mathbf{x}\in\Omega:\phi^m<\delta_1\}\subset\{\mathbf{x}\in\Omega:\phi^m<\delta_2\}\subset\cdots\subset\{\mathbf{x}\in\Omega:\phi^m<\delta_n\}\subset\cdots$ and $\cup_{n=1}^\infty\{\mathbf{x}\in\Omega:\phi^m<\delta_n\}=\{\mathbf{x}\in\Omega:\phi<\delta\}$, by the monotone set theorem,

$$|\{\mathbf{x}\in\Omega:\phi<\delta\}|=\lim_{n\to\infty}|\{\mathbf{x}\in\Omega:\phi^m<\delta_n\}|\leq V.$$

Similarly, since there exists $\hat{\delta}_1\geq\hat{\delta}_2\geq\cdots\geq\hat{\delta}_n\cdots$, $\hat{\delta}_n\to\delta$ and $|\{\mathbf{x}\in\Omega:\phi^m<\hat{\delta}_n\}|\geq V$. We have

$$|\{\mathbf{x}\in\Omega:\phi\leq\delta\}|=\lim_{n\to\infty}|\{\mathbf{x}\in\Omega:\phi^m<\hat{\delta}_n\}|\geq V.$$

Therefore, $\tilde{A}_\delta$ exists.

Denote

$$\underline{A}_\delta=\{\mathbf{x}\in\Omega:\phi^m(\mathbf{x})<\delta\}, \quad A_\delta=\{\mathbf{x}\in\Omega:\phi^m(x)=\delta\} \quad \text{and} \quad \overline{A}_\delta=\{\mathbf{x}\in\Omega:\phi^m(\mathbf{x})>\delta\}.$$

Note for any $\chi\in B$, we have

$$(\chi^{m+1}(\mathbf{x})-\chi(\mathbf{x}))\phi^m(\mathbf{x})\leq(\chi^{m+1}(\mathbf{x})-\chi(\mathbf{x}))\delta$$

by considering the following situations of $\mathbf{x}$:

$$\begin{aligned}
&\chi^{m+1}(\mathbf{x})=1, \quad \rho(\mathbf{x})\leq 1, \quad \chi(\mathbf{x})-\chi^{m+1}(\mathbf{x})\leq 0, \quad \chi^m(\mathbf{x})<\delta, && \text{when } \mathbf{x}\in\underline{A}_\delta,\\
&\chi^m(\mathbf{x})=\delta, && \text{when } \mathbf{x}\in A_\delta,\\
&\chi^{m+1}(\mathbf{x})=0, \quad \rho(\mathbf{x})\geq 0, \quad \chi(\mathbf{x})-\chi^{m+1}(\mathbf{x})\geq 0, \quad \chi^m(\mathbf{x})>\delta, && \text{when } \mathbf{x}\in\overline{A}_\delta.
\end{aligned}$$

Therefore,

$$\int_\Omega \chi^{m+1}\phi^m d\mathbf{x}-\int_\Omega \chi\phi^m d\mathbf{x}=\int_\Omega(\chi^{m+1}-\chi)\phi^m d\mathbf{x}\leq\delta\left(\int_\Omega\chi^{m+1}d\mathbf{x}-\int_\Omega\chi d\mathbf{x}\right).$$

If

$$\int_\Omega\chi d\mathbf{x}=V=\int_\Omega\chi^{m+1}d\mathbf{x}, \quad \delta\left(\int_\Omega\chi^{m+1}d\mathbf{x}-\int_\Omega\chi d\mathbf{x}\right)=0,$$

and thus

$$\int_\Omega\chi^{m+1}\phi^m d\mathbf{x}-\int_\Omega\chi\phi^m d\mathbf{x}\leq 0.$$

If

$$\delta\leq 0, \quad \delta\left(\int_\Omega\chi^{m+1}d\mathbf{x}-\int_\Omega\chi d\mathbf{x}\right)\leq 0, \quad \forall\chi\in B,$$

since for any $\chi\in B$, we have

$$V=\int_\Omega\chi^{m+1}d\mathbf{x}\geq\int_\Omega\chi d\mathbf{x}.$$

This completes the proof. □

Theorem 4.1. *For any $\sigma>0$, $\mathcal{J}(\chi,\mathbf{R})$ is nonincreasing in each iteration of χ and $\mathbf{R}$ in Algorithm* 3.1. *That is, $\forall m\geq 1$,*

$$\mathcal{J}(\chi^{m+1},\mathbf{R}^m)\leq\mathcal{J}(\chi^m,\mathbf{R}^m)\leq\mathcal{J}(\chi^m,\mathbf{R}^{m-1}).$$

Proof. By Lemma 2.1,

$$\mathbf{R}^{m-1}=k(G_\sigma*\chi^{m-1})\nabla T^{m-1}\in S, \quad \mathbf{R}^m=k(G_\sigma*\chi^m)\nabla T^m=\underset{\mathbf{R}\in S}{\arg\min}\,\mathcal{J}(\chi^m,\mathbf{R}).$$

Therefore,

$$\mathcal{J}(\chi^m,\mathbf{R}^m)\leq\mathcal{J}(\chi^m,\mathbf{R}^{m-1}).$$

Note

$$\begin{aligned}\mathcal{J}(\chi,\mathbf{R}^m)&=\int_\Omega\left[\frac{1}{k_0}+\left(\frac{1}{k_1}-\frac{1}{k_0}\right)G_\sigma*\chi\right]\mathbf{R}^m\cdot\mathbf{R}^m d\mathbf{x}\\&=\text{constant}+\int_\Omega\left(\frac{1}{k_0}-\frac{1}{k_1}\right)(G_\sigma*\chi)\mathbf{R}^m\cdot\mathbf{R}^m d\mathbf{x}\\&=\text{constant}+\int_\Omega\chi G_\sigma*\left[\left(\frac{1}{k_0}-\frac{1}{k_1}\right)\mathbf{R}^m\cdot\mathbf{R}^m\right]d\mathbf{x}\\&=\text{constant}+\int_\Omega\chi\phi^m d\mathbf{x}.\end{aligned}$$

By Lemma 4.1,

$$\int_\Omega\chi^m d\mathbf{x}=\int_\Omega\chi^{m+1}d\mathbf{x}=V\quad\text{ and }\quad\int_\Omega\chi^{m+1}\phi^m d\mathbf{x}\le\int_\Omega\chi^m\phi^m d\mathbf{x}.$$

Therefore,

$$\mathcal{J}(\chi^{m+1},\mathbf{R}^m)\le\mathcal{J}(\chi^m,\mathbf{R}^m).$$

This completes the proof. □

5 Numerical implementation

We discretize the rectangular domain $\Omega=\{(x,y)|a_1\le x\le a_2,\ b_1\le y\le b_2\}$ into uniform squares with side length h and sides parallel to the coordinate axes. Denote the collection of all open uniform squares as $\mathcal{S}_h$. On each square, the characteristic function χ_h is assumed to be constant and the temperature T_h is bilinear, that is,

$$\begin{aligned}&\chi_h\in\{\chi:\Omega\to\{0,1\}|\chi_h|_e=0,\text{ or }\chi_h|_e=1,\ \forall e\in\mathcal{S}_h\}.\\&T_h\in W_h:=\{T\in H^1(\Omega,\mathbb{R})|T|_K\in Q(\bar{e}),\ \forall e\in\mathcal{S}_h\},\end{aligned}$$

where $\bar{e}$ is the closure of e and the bilinear function space $Q=\{c_1xy+c_2x+c_3y+c_4,c_1,c_2,c_3,c_4\in\mathbb{R}\}$. To let T_h satisfy the Dirichlet boundary condition, additionally

$$T_h\in W_h^D:=\{T\in W_h|T|_{\Gamma_D}=T_0\}.$$

An approximation of the solution to (2.1b) in W_h^D solves

$$\int_\Omega k\nabla T_h\nabla P_h d\mathbf{x}=\int_\Omega qP_h d\mathbf{x},\quad\forall P_h\in W_h^D,$$

where $k=k(\rho_h)$ and $\rho_h\in\{\rho:\Omega\to[0,1]|\rho|_e\in P_0(e),\ \forall e\in\mathcal{S}_h\}$ approximates the convolution $G_\sigma*\chi$ by a weighted average. Concretely,

$$\rho_h|_e=\sum_{|i|\le r,|j|\le r} g_{(i,j)}\chi_h|_{e+(i,j)},$$
$$g_{(i,j)}=Ce^{-\frac{i^2+j^2}{2\sigma^2}h^2},$$

where $e+(i,j)$ is the element defined by $\{(x+ih,y+jh)|(x,y)\in e\}$ and C is the normalization factor to enforce

$$\sum_{|i|\le r,\ |j|\le r} g_{(i,j)}=1.$$

After solving for T_h, we could find $\mathbf{R}_h\in\{R:\Omega\to\mathbb{R}^2|R|_e\in P_1(e),\ e\in\mathcal{S}_h\}$ and the objective functional as follows,

$$\mathbf{R}_h|_e=k(\rho_h|_e)\nabla T_h,\quad \forall e\in\mathcal{S}_h,$$
$$\mathcal{J}_h=\int_\Omega\frac{1}{k(\rho_h)}\mathbf{R_h}\mathbf{R_h}d\mathbf{x}=\sum_{e\in\mathcal{S}_h}\left[\left(\frac{1}{k_1}-\frac{1}{k_0}\right)\rho_h|_e+\frac{1}{k_0}\right]\int_e\mathbf{R}_h\mathbf{R}_hd\mathbf{x}$$
$$=\sum_{e\in\mathcal{S}_h}\chi_h|_e\left[\left(\frac{1}{k_1}-\frac{1}{k_0}\right)\sum_{|i|\le r,|j|\le r}g_{(i,j)}\int_{e+(i,j)}\mathbf{R}_h\mathbf{R}_hd\mathbf{x}\right]+\frac{1}{k_0}\sum_{e\in\mathcal{S}_h}\int_e\mathbf{R}_h\mathbf{R}_hd\mathbf{x}.$$

χ_h is then updated according to ϕ_h which is elementwise defined as

$$\phi_h|_e=\left(\frac{1}{k_1}-\frac{1}{k_0}\right)\sum_{|i|\le r,|j|\le r}g_{(i,j)}\int_{e+(i,j)}\mathbf{R}_h\mathbf{R}_hd\mathbf{x},\quad\forall e\in\mathcal{S}_h.$$

Let M be the largest integer so that $Mh^2\le V$. The new χ_h takes 1 on the elements corresponding to M smallest element values of ϕ_h and 0 elsewhere.

6 Numerical experiments

In this section, we test our algorithm on two examples. The first is the volume-to-point problem considered by Bejan [2], in which the high conductive material conducts heat uniformly generated in the volume to a point heat sink on the boundary. We approximate the point by a short isothermal boundary as in [8]. The second is the volume-to-sides problem, where the plate is surrounded by isothermal boundary which is considered in [11].

6.1 Volume-to-point problem

We consider a unit square plate with side length $A=1$ as shown in Fig. 1. The heat is generated uniformly over the plate. It is surrounded by adiabatic boundaries. The only way to cool the plate down is to conduct heat to a short isothermal boundary with length C on the middle of the bottom side, on which $T=T_0$. Since we are concerned about $\int_\Omega k\nabla T\cdot\nabla T d\mathbf{x}$, the value of T_0 does not affect the computational results. For simplicity we let $T_0=0$. We also let the quantity $\frac{q}{k_0}=50$.

Due to symmetry, we only need to compute the right half of the domain. On the line of symmetry, the temperature satisfies the Neumann boundary condition. We always use a uniform initial distribution. The convergence criterion is that $||\chi_h^n-\chi_h^{n-1}||_{L^1}<1e-4$. The maximum number of iterations required to meet the convergence criterion for the experiments in this subsection is 205 and the average number of iterations is 108.1. Fig. 2 shows the optimal designs for $\sigma=2.5\times10^{-3}$ and with different resolutions. We can see that the overall topology of the distribution is quite stable when mesh is refined. The distribution looks like a tree with branches extending to the adiabatic boundaries. The results with a half of the $\sigma=1.25\times10^{-3}$ are shown in Fig. 3. In this case, the branches are finer with smaller σ compared to those in Fig. 2. We could still see from the figure that the overall topology is relatively stable when mesh is refined. Fig. 4 verifies the energy decaying property of our algorithm. We show the case when the volume fraction is 0.2, $k_1/k_0=500$,

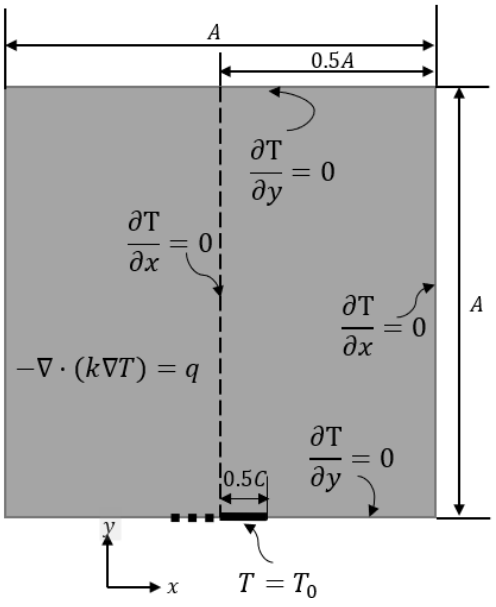

Figure 1: The volume-to-point problem.

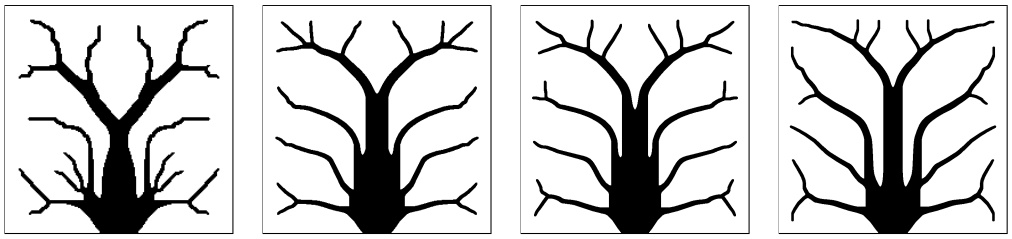

Figure 2: Mesh resolution $=200\times200,500\times500,700\times700,800\times800$ from left to right. Volume fraction $=0.2$, $\sigma=2.5\times10^{-3}$, $\frac{k_1}{k_0}=500$, $C=0.05$.

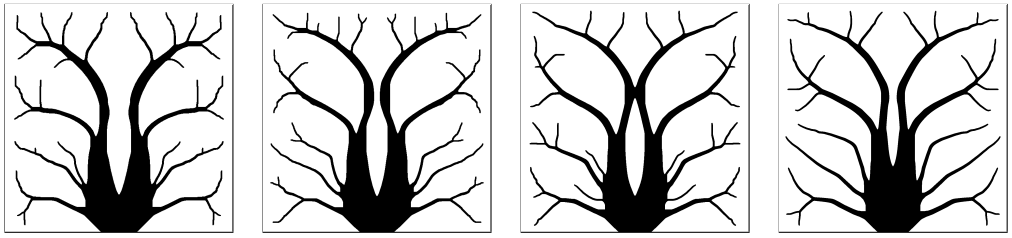

Figure 3: Mesh resolution $=700\times700,800\times800,950\times950,1300\times1300$ from left to right. Volume fraction $=0.2$, $\sigma=1.25\times10^{-3}$, $\frac{k_1}{k_0}=500$, $C=0.05$.

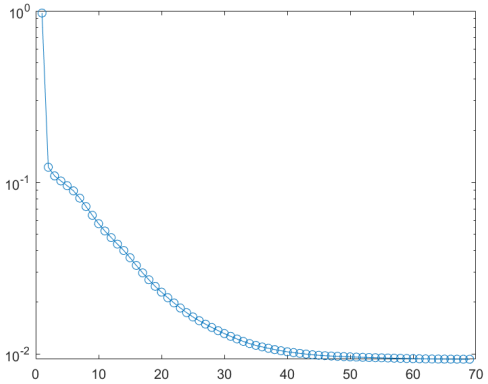

Figure 4: The objective versus the number of iterations. Volume fraction$=0.2$, Mesh resolution 500×500, $\sigma=2.5\times10^{-3}$, $\frac{k_1}{k_0}=500$.

and $\sigma=2.5\times10^{-3}$. The objective functional decays in each iteration. All other experiments could also produce similar energy curves.

Fig. 5 shows the optimized distribution as the volume fraction (of the high conducting material) increases. The volume distribution tends to concentrate on the tree trunk, especially close to the isothermal boundary while the thickness of the

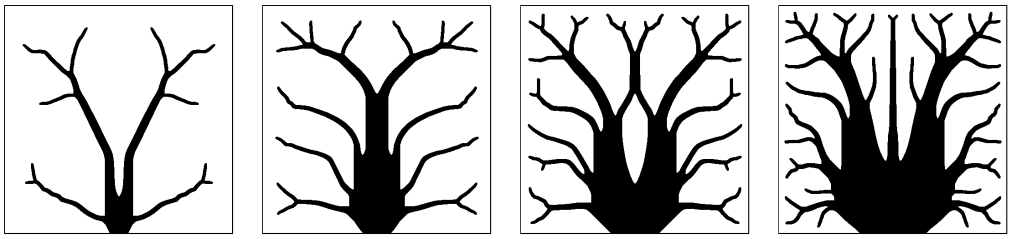

Figure 5: Volume fraction $=0.1$, 0.2, 0.3, 0.4 from left to right. Mesh resolution 500×500, $\sigma=2.5\times10^{-3}$, $\frac{k_1}{k_0}=500$, $C=0.05$.

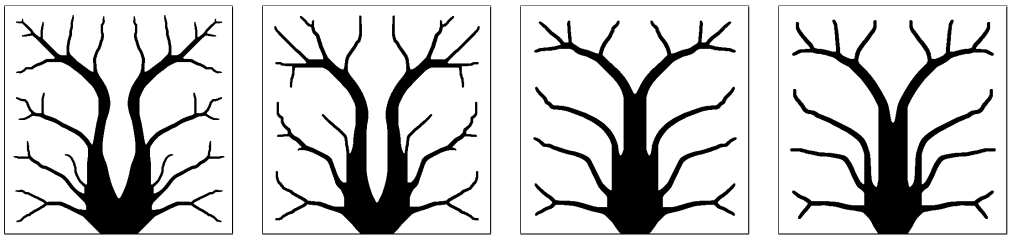

Figure 6: $\sigma=1.5\times10^{-4},2\times10^{-3},2.5\times10^{-3},3\times10^{-3}$ from left to right. Volume fraction $=0.2$, mesh resolution 500×500, $\frac{k_1}{k_0}=500$, $C=0.05$.

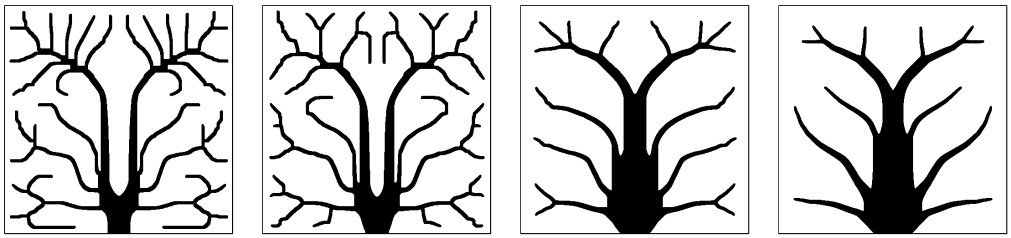

Figure 7: $\frac{k_1}{k_0}=50000,10000,500,100$ from left to right. Volume fraction$=0.2$, mesh resolution 500×500, $\sigma=1.25\times10^{-3}$, $C=0.05$.

smallest branches seems unchanged. When the volume fraction is the same, the optimized distribution depends on filter size σ and conductivity ratio $\frac{k_1}{k_0}$. In Fig. 6, when σ becomes larger, we can see that the distribution contains less fine branches. This is because after convolution with G_σ the fine branches will have lower conducting efficiency when σ is larger. Similarly when $\frac{k_1}{k_0}$ becomes smaller, thin branches conduct heat less efficiently compared to when $\frac{k_1}{k_0}$ is large. As shown in Fig. 7, as $\frac{k_1}{k_0}$ becomes smaller, branches becomes thicker.

6.2 Volume-to-sides problem

Here we consider a square plate all of whose boundary is isothermal with $T=T_0$ as shown in Fig. 8. Inside the plate, heat is generated uniformly. Due to symmetry, we only optimize over the upper left quadrant of the plate. On the vertical line and the horizonal line of symmetry (dashed lines in Fig. 8), we impose Neumann boundary conditions on T. We set volume fraction to be 0.5 and $A=1$. $T_0=0$ and $\frac{q}{k_0}=50$. The initial distribution is uniform and the convergence criterion is the same as that for the volume-to-point problem. The average number of iterations for the experiments presented here is 150.9. The results for different mesh resolution are shown in Fig. 9. The distribution of the void region (white region) looks like a leaf in each quadrant of the plate. As the mesh is refined, the distribution stabilizes. Fig. 10 shows that as the volume fraction of high conductive material increases, mainly those parts close to the vertical and horizontal symmetric lines of the plate get thickened, which effectively transfer heat generated in the center to the isothermal boundaries. The influence of the conductivity ratio $\frac{k_1}{k_0}$ and the filter size σ to the optimized distribution can be seen in Fig. 11 and in Fig. 12 respectively. Similar to the volume-to-point problem, the results exhibit finer structures when the conductivity ratio becomes larger or the filter size becomes smaller.

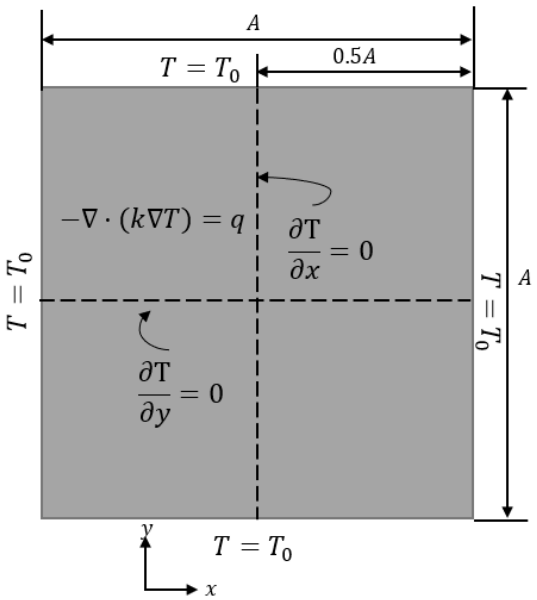

Figure 8: The volume-to-sides problem.

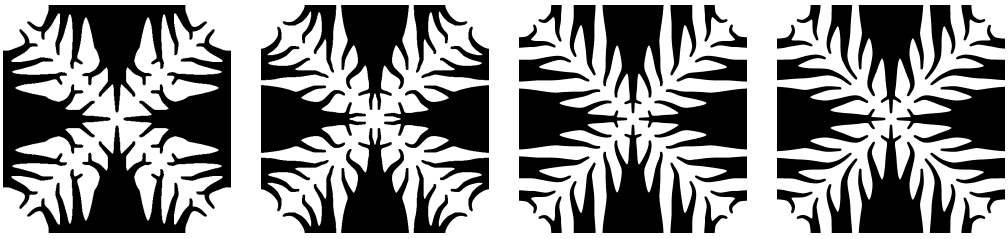

Figure 9: From left to right, mesh resolution is 500×500, 600×600, 1400×1400, 1600×1600. $\frac{k_1}{k_0}=100$,$\sigma=2.5\times10^{-3}$. Volume-to-sides problem.

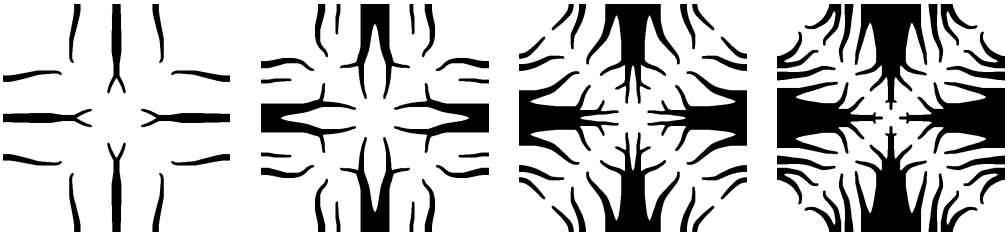

Figure 10: From left to right, volume fraction $=0.1$,0.2,0.3,0.4. $\sigma=2.5\times10^{-3}$, $\frac{k_1}{k_0}=100$. Mesh resolution is 600×600.

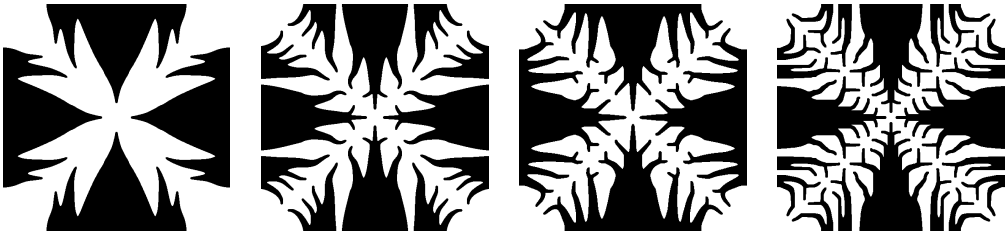

Figure 11: From left to right, $\frac{k_1}{k_0}=10$,50,100,500. Mesh resolution is 600×600. $\sigma=2.5\times10^{-3}$. Volume-to-sides problem.

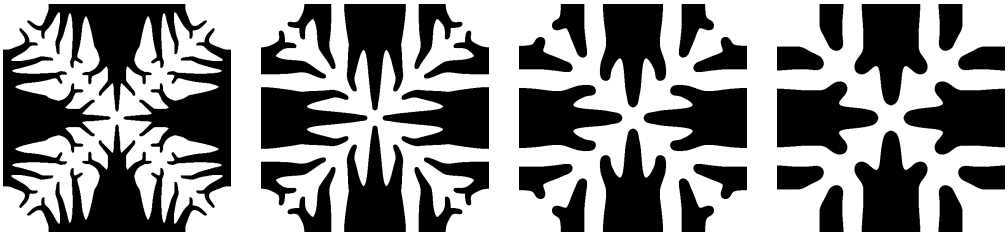

Figure 12: From left to right, $\sigma=2.5\times10^{-3}$,5×10^{-3},1×10^{-2},2×10^{-2}. Mesh resolution is 600×600. $\frac{k_1}{k_0}=500$. Volume-to-sides problem.

7 Conclusions

By reformulating the heat transfer problem into a min-min problem, we developed a volume-preserving coordinate descent method, in which the characteristic function is updated by an iterative thresholding method. The method is simple to use and has the energy decaying property. The characteristic function gives a black-or-white design without need of post-processing. Numerical experiments are conducted to show the efficiency of the method. We also studied the effects of the conductivity ratio and filter size on the optimized distributions.

Appendix: Proof of Lemma 2.1

Proof. It is easy to see that $\mathbf{R}^*=k\nabla T\in S$ by (2.1b) and the definition of S. We also have

$$\int_\Omega \frac{1}{k}\mathbf{R}^*\cdot\mathbf{R}^*d\mathbf{x}=\int_\Omega \frac{1}{k}k\nabla T\cdot k\nabla T d\mathbf{x}=\int_\Omega k\nabla T\cdot\nabla T d\mathbf{x}.$$

Now we show that R^* minimizes $\int_\Omega \frac{1}{k}\mathbf{R}\cdot\mathbf{R}d\mathbf{x}$ over S. $\forall\mathbf{R}\in S$,

$$\begin{aligned}&\int_\Omega \frac{1}{k}\mathbf{R}^*\cdot\mathbf{R}^*d\mathbf{x}-\int_\Omega \frac{1}{k}\mathbf{R}\cdot\mathbf{R}d\mathbf{x}\\ =&\int_\Omega \frac{1}{k}(\mathbf{R}^*-\mathbf{R})\cdot(\mathbf{R}^*+\mathbf{R})d\mathbf{x}\\ =&\int_\Omega \frac{1}{k}(\mathbf{R}^*-\mathbf{R})\cdot(\mathbf{R}-\mathbf{R}^*)d\mathbf{x}+2\int_\Omega \frac{1}{k}(\mathbf{R}^*-\mathbf{R})\cdot\mathbf{R}^*d\mathbf{x}.\end{aligned}$$

Substituting $\mathbf{R}^*$ with $k\nabla T$ first and then integrating by parts, we have

$$\begin{aligned}\int_\Omega \frac{1}{k}(\mathbf{R}^*-\mathbf{R})\cdot\mathbf{R}^*d\mathbf{x}=&\int_\Omega (\mathbf{R}^*-\mathbf{R})\cdot\nabla T d\mathbf{x}\\ =&\int_\Gamma (T-T_0)(\mathbf{R}^*-\mathbf{R})\cdot\mathbf{n}ds-\int_\Omega \nabla\cdot(\mathbf{R}^*-\mathbf{R})(T-T_0)d\mathbf{x}. \quad (A.1)\end{aligned}$$

Since $T=T_0$ on Γ_D, $\mathbf{R}\cdot\mathbf{n}=\mathbf{R}^*\cdot\mathbf{n}=0$ on $\Gamma\backslash\Gamma_D$, $\nabla\cdot\mathbf{R}^*=\nabla\cdot\mathbf{R}$ in Ω,

$$\int_\Omega \frac{1}{k}(\mathbf{R}^*-\mathbf{R})\cdot\mathbf{R}^*d\mathbf{x}=0.$$

Therefore,

$$\int_\Omega \frac{1}{k}\mathbf{R}^*\cdot\mathbf{R}^*d\mathbf{x}-\int_\Omega \frac{1}{k}\mathbf{R}\cdot\mathbf{R}d\mathbf{x}=\int_\Omega \frac{1}{k}(\mathbf{R}^*-\mathbf{R})\cdot(\mathbf{R}-\mathbf{R}^*)d\mathbf{x}\leq 0.$$

This completes the proof. □

Acknowledgements

X.-P. Wang acknowledges support from National Natural Science Foundation of China (NSFC) grant (No. 12271461), the key project of NSFC (No. 12131010), the Hong Kong Research Grants Council GRF (GRF grants Nos. 16308421, 16305819, 16303318) and the University Development Fund from The Chinese University of Hong Kong, Shenzhen (UDF01002028).

References

[1] Joe Alexandersen, Ole Sigmund, and Niels Aage, Large scale three-dimensional topology optimisation of heat sinks cooled by natural convection, Int. J. Heat Mass Transf., 100 (2016), 876–891.

[2] Adrian Bejan, Constructal-theory network of conducting paths for cooling a heat generating volume, Int. J. Heat Mass Transf, 40(4) (1997), 799–816.

[3] Francois H. Burger, Jaco Dirker, and Josua P. Meyer, Three-dimensional conductive heat transfer topology optimisation in a cubic domain for the volume-to-surface problem, Int. J. Heat Mass Transf, 67 (2013), 214–224.

[4] Luyu Cen, Wei Hu, Dong Wang, and Xiaoping Wang, An iterative thresholding method for the minimum compliance problem, Commun. Comput. Phys., 33(4) (2023), 1189–1216.

[5] Huangxin Chen, Haitao Leng, Dong Wang, and Xiao-Ping Wang, An efficient threshold dynamics method for topology optimization for fluids, CSIAM Trans. Appl. Math., 3(1) (2022), 26–56.

[6] Talib Dbouk, A review about the engineering design of optimal heat transfer systems using topology optimization, Appl. Thermal Eng., 112 (2017), 841–854.

[7] Ercan M. Dede, Yanghe Liu, Shailesh N. Joshi, Feng Zhou, Danny J. Lohan, and Jong-Won Shin, Optimal design of three-dimensional heat flow structures for power electronics applications, J. Thermal Sci. Eng. Appl., 11(2) (2019).

[8] Jaco Dirker and Josua P. Meyer, Topology optimization for an internal heat-conduction cooling scheme in a square domain for high heat flux applications, J. Heat Transf., 135(11) (2013).

[9] Selim Esedoglu and Felix Otto, Threshold dynamics for networks with arbitrary surface tensions, Commun. Pure Appl. Math., 68(5) (2014), 808–864.

[10] Ahmad Fawaz, Yuchao Hua, Steven Le Corre, Yilin Fan, and Lingai Luo, Topology optimization of heat exchangers: A review, Energy, (2022), 124053.

[11] Allan Gersborg-Hansen, Martin P. Bendsøe, and Ole Sigmund, Topology optimization of heat conduction problems using the finite volume method, Struct. Multidiscip. Optim., 31 (2006), 251–259.

[12] Wei Hu, Dong Wang, and Xiao-Ping Wang, An efficient iterative method for the formulation of flow networks, Commun. Comput. Phys., 31(5) (2022), 1317–1340.

[13] Guoxian Jing, Hiroshi Isakari, Toshiro Matsumoto, Takayuki Yamada, and Toru Takahashi, Level set-based topology optimization for 2d heat conduction problems using bem with objective function defined on design-dependent boundary with heat transfer boundary condition, Eng. Anal. Bound. Elem., 61 (2015), 61–70.

[14] Adriano A. Koga, Edson Comini C. Lopes, Helcio F. Villa Nova, Cícero R. De Lima, and Emílio Carlos Nelli Silva, Development of heat sink device by using topology optimization, Int. J. Heat Mass Transf., 64 (2013), 759–772.

[15] Sina Lohrasbi, René Hammer, Werner Essl, Georg Reiss, Stefan Defregger, and Wolfgang Sanz, A comprehensive review on the core thermal management improvement concepts in power electronics, Ieee Access, 8 (2020), 166880–166906.

[16] Barry Merriman, James Kenyard Bence, and Stanley Osher, Diffusion Generated Motion by Mean Curvature, volume 27, Department of Mathematics, University of California, Los Angeles, 1992.

[17] Gilberto Moreno, Sreekant Narumanchi, Xuhui Feng, Paul Anschel, Steve Myers, and Phil Keller, Electric-drive vehicle power electronics thermal management: Current status, challenges, and future directions, J. Electronic Packag., 144(1) (2022).

[18] Chayan Nadjahi, Hasna Louahlia, and Stéphane Lemasson, A review of thermal management and innovative cooling strategies for data center, Sustainable Computing: Informatics and Systems, 19 (2018), 14–28.

[19] Alberto Pizzolato, Ashesh Sharma, Kurt Maute, Adriano Sciacovelli, and Vittorio Verda, Topology optimization for heat transfer enhancement in latent heat thermal energy storage, Int. J. Heat Mass Transf, 113 (2017), 875–888.

[20] Yasuyuki Sakai, Hiroshi Ishiyama, and Takaji Kikuchi, Power control unit for high power hybrid system, Technical report, SAE Technical Paper, 2007.

[21] V. Subramaniam, T. Dbouk, and J.-L. Harion, Topology optimization of conductive heat transfer devices: An experimental investigation, Appl. Thermal Eng., 131 (2018), 390–411.

[22] Dong Wang, Haohan Li, Xiaoyu Wei, and Xiao-Ping Wang, An efficient iterative thresholding method for image segmentation, J. Comput. Phys., 350 (2017), 657–667.

[23] Dong Wang and Xiao-Ping Wang, The iterative convolution–thresholding method (ictm) for image segmentation, Pattern Recognition, (2022), 108794.

[24] Yongcun Zhang and Shutian Liu, Design of conducting paths based on topology optimization, Heat Mass Transf., 44 (2008), 1217–1227.

[25] Chungang Zhuang, Zhenhua Xiong, and Han Ding, A level set method for topology optimization of heat conduction problem under multiple load cases, Comput. Methods Appl. Mech. Eng., 196(4-6) (2007), 1074–1084.